

THE EVOLUTION OF THE $M_{\text{BH}}\text{-}\sigma$ RELATION

BRANT ROBERTSON,¹ LARS HERNQUIST,¹ THOMAS J. COX,¹ TIZIANA DI MATTEO,² PHILIP F. HOPKINS,¹
PAUL MARTINI,¹ AND VOLKER SPRINGEL³

Received 2005 June 1; accepted 2005 December 6

ABSTRACT

We examine the evolution of the black hole mass–stellar velocity dispersion ($M_{\text{BH}}\text{-}\sigma$) relation over cosmic time, using simulations of galaxy mergers that include feedback from supermassive black hole growth. For a range in redshifts $z = 0\text{--}6$, we modify the virial mass, gas fraction, interstellar medium equation of state, surface mass density, and concentration of dark matter halos of the merger progenitors to match those expected at various cosmic times. We find that the slope of the $M_{\text{BH}}\text{-}\sigma$ relation is insensitive to the redshift-dependent properties of merger progenitors and should be roughly constant at redshifts $z = 0\text{--}6$. For the same feedback efficiency that reproduces the observed amplitude of the $M_{\text{BH}}\text{-}\sigma$ relation at $z = 0$, there is a weak redshift dependence to the normalization, corresponding to an evolution in the Faber-Jackson relation, which results from an increasing velocity dispersion for a given galactic stellar mass. We develop a formalism to connect redshift evolution in the $M_{\text{BH}}\text{-}\sigma$ relation to the scatter in the local relation at $z = 0$. For an assumed model for the accumulation of black holes with different masses over cosmic time, we show that the scatter in the local relation places severe constraints on the redshift evolution of both the normalization and slope of the $M_{\text{BH}}\text{-}\sigma$ relation. Furthermore, we demonstrate that the cosmic downsizing of the black hole population introduces a black hole mass–dependent dispersion in the $M_{\text{BH}}\text{-}\sigma$ relation and that the skewness of the distribution about the locally observed $M_{\text{BH}}\text{-}\sigma$ relation is sensitive to redshift evolution in the normalization and slope. In agreement with existing constraints, our simulations imply that hierarchical structure formation should produce the relation with small intrinsic scatter, as the physical origin of the $M_{\text{BH}}\text{-}\sigma$ enjoys a remarkable resiliency to the redshift-dependent properties of merger progenitors.

Subject headings: black hole physics — galaxies: evolution — galaxies: formation

1. INTRODUCTION

Galactic spheroids exhibit a constitutive relation between their stellar kinematics and supermassive black holes (SMBHs) through observed correlations between black hole mass M_{BH} and either the bulge mass M_{bulge} (Miyoshi et al. 1995; Kormendy & Richstone 1995; Eckart & Genzel 1997; Faber et al. 1997; Magorrian et al. 1998; Ghez et al. 1998) or the velocity dispersion σ ($M_{\text{BH}}\text{-}\sigma$; Ferrarese & Merritt 2000; Gebhardt et al. 2000). The $M_{\text{BH}}\text{-}\sigma$ relation locally is a tight, power-law correlation with a logarithmic slope originally estimated to be in the range $\beta \approx 3.75\text{--}4.8$ (Ferrarese & Merritt 2000; Gebhardt et al. 2000). Later studies improved the accuracy of the local correlation (e.g., Tremaine et al. 2002, hereafter T02) and explored the relation between SMBH mass and other galaxy properties more fully (Wandel 2002; Ferrarese 2002; Marconi & Hunt 2003; Bernardi et al. 2003; Baes et al. 2003). Efforts to extend our knowledge of the connection between SMBHs and their host galaxies to higher redshifts include attempts to measure SMBH properties at $z = 4\text{--}6$ (Vestergaard 2004) and to quantify the relation between SMBHs and galaxy kinematics in distant, active galaxies (Shields et al. 2003; Treu et al. 2004; Walther et al. 2004).

Observations of active galaxies at $z > 0$ have yielded ambiguous inferences about the nature of the $M_{\text{BH}}\text{-}\sigma$ at other redshifts, implying both redshift-dependent (Treu et al. 2004; Walther et al. 2004) and redshift-independent relations (Shields et al. 2003). Knowledge of the $M_{\text{BH}}\text{-}\sigma$ relation over cosmological time is

crucial to understanding galaxy formation if SMBH feedback has a significant impact on this process (e.g., Springel et al. 2005a; Robertson et al. 2006). The focus of our present work is to characterize the development of the $M_{\text{BH}}\text{-}\sigma$ relation over cosmic time with a large set of hydrodynamic simulations of galaxy mergers that include star formation and feedback from the growth of SMBHs, to use existing data to constrain redshift evolution in the $M_{\text{BH}}\text{-}\sigma$ relation, and to motivate specific observational tests for the $M_{\text{BH}}\text{-}\sigma$ relation at high redshifts, using the next generation of large telescopes.

A variety of theoretical models have been proposed to explain the $M_{\text{BH}}\text{-}\sigma$ relation, based on physical mechanisms such as viscous disk accretion (Burkert & Silk 2001), adiabatic black hole growth (MacMillan & Henriksen 2002), gas or dark matter collapse (Adams et al. 2001; Balberg & Shapiro 2002; Adams et al. 2003), stellar capture by accretion disks (Miralda-Escudé & Kollmeier 2005), dissipationless merging (Ciotti & van Albada 2001; Nipoti et al. 2003), unregulated gas accretion (Archibald et al. 2002; Kazantzidis et al. 2005), and the self-regulated growth of black holes by momentum- or pressure-driven winds (Silk & Rees 1998; King 2003; Murray et al. 2005; Di Matteo et al. 2005; Sazonov et al. 2005). An important outcome of these studies has been the recognition that the growth of SMBHs may have important consequences cosmologically, especially for galaxy formation, motivating work linking the hierarchical growth of structure with the evolution or demographics of SMBHs through studies of quasar evolution (Haiman & Loeb 1998; Richstone et al. 1998; Fabian 1999; Monaco et al. 2000; Kauffmann & Haehnelt 2000; Haehnelt & Kauffmann 2000; Granato et al. 2001; Menou et al. 2001; Menci et al. 2003; Di Matteo et al. 2003, 2004; Wyithe & Loeb 2003; Wyithe 2006; Hopkins et al. 2005a, 2005b, 2005c, 2005d) and the formation of normal galaxies (Volonteri et al. 2003; Cox et al. 2006; Robertson et al. 2006).

¹ Harvard-Smithsonian Center for Astrophysics, 60 Garden Street, Cambridge, MA 02138; brobertson@cfa.harvard.edu.

² Department of Physics, Carnegie Mellon University, 5000 Forbes Avenue, Pittsburgh, PA 15213.

³ Max-Planck-Institut für Astrophysik, Karl-Schwarzschildstrasse 1, 85740 Garching bei München, Germany.

Motivated by the long-standing view that mergers form spheroids (e.g., Toomre 1977), Di Matteo et al. (2005) studied the self-regulated growth of black holes in galaxy collisions and showed that this process can reproduce the $M_{\text{BH}}-\sigma$ relation at $z = 0$ for progenitors similar to local galaxies. The work of Di Matteo et al. (2005) served as an important early attempt to calculate the effects of black hole growth and feedback on the process of galaxy formation by addressing the generation of an $M_{\text{BH}}-\sigma$ relation in self-consistent hydrodynamical simulations. This calculation has served as a foundation for proceeding research that has attempted to explore the emerging paradigm that SMBH formation is a natural and essential outcome of hierarchical spheroid formation. Springel et al. (2005a) calculated the role of active galactic nucleus (AGN) feedback in the reddening spheroids formed in mergers by truncating residual star formation. Robertson et al. (2006) explored the effects of AGN feedback in reducing the size of spheroids of disk galaxies forming in the early gas-rich environments of high redshifts. Cox et al. (2006) calculated the contribution of AGN outflows to the X-ray emission from halo gas in elliptical galaxies. Importantly, Hopkins et al. (2005a, 2005b, 2005c, 2005d, 2006a, 2006b, 2006c) calculated a wide range of implications of the co-evolution of spheroids and black holes for the interpretation of both quasar and galaxy observations. Hopkins et al. (2005a, 2005b, 2005c, 2005d) demonstrated that modeling the obscured growth of black holes during gas-rich galaxy mergers leads to a luminosity-dependent quasar lifetime that differs substantially from standard assumptions for the time dependence of quasar activity. The luminosity-dependent quasar lifetime leads naturally to a new interpretation of the quasar luminosity function, in which low-luminosity quasars are primarily massive black holes in sub-Eddington accretion phases, while quasars with luminosities above the break in the quasar luminosity function are accreting near the Eddington rate. Hopkins et al. (2006a, hereafter H06a) showed that the luminosity-dependent lifetime and the new interpretation of the quasar luminosity function can explain a wide variety of quasar observations by deconvolving the growing black hole population from the hard X-ray luminosity function, including longer wavelength quasar luminosity functions, the spectrum of the X-ray background, and the obscured fraction of quasars as a function of quasar luminosity. The model presented in H06a also leads to a new model for quasar clustering (Lidz et al. 2006) and predictions for the evolution of the faint-end slope of the quasar luminosity function (Hopkins et al. 2006b). Furthermore, Hopkins et al. (2006c) showed that the co-evolution of spheroids and black holes in these hydrodynamical models can account for the evolution of the red galaxy sequence, building off the previous calculations of Springel et al. (2005a) and H06a.

Many of the previously mentioned calculations use knowledge of the connection between SMBHs and their host spheroids over cosmological time and throughout the process of hierarchical structure formation. The calculations presented in this paper provide a detailed hydrodynamical calculation of the nature of this spheroid–black hole connection, using cosmologically motivated galaxy models at a variety of redshifts, and have already served as essential input into many of the aforementioned calculations. Independently, the detailed calculation of the $M_{\text{BH}}-\sigma$ relation with redshift provides an important method for testing the premise of spheroidal galaxy formation through the hierarchical merging of galaxies against observational constraints from the $M_{\text{BH}}-\sigma$ relation observed locally and at high redshifts. These calculations will also serve as a basis for future comparisons between theoretical expectations for the co-evolution of black holes and spheroids with observations of ultraluminous infrared gal-

axies (e.g., Sanders et al. 1988; Sanders & Mirabel 1996) and the submillimeter emission from galaxies observed with the Submillimeter Common-User Bolometric Array (SCUBA; e.g., Smail et al. 1997).

Specifically, in this paper we use the Di Matteo et al. (2005) model to explicitly calculate the behavior of the $M_{\text{BH}}-\sigma$ relation with cosmic time induced by the redshift scalings of galaxy properties. Using a large set of hydrodynamical simulations of mergers that include feedback from supernovae and accreting SMBHs, the resulting $M_{\text{BH}}-\sigma$ relation is calculated for galaxy models that span a large range in virial mass, gas fraction, interstellar medium equation of state (EOS), surface mass density, dark matter concentration, and redshift.

We determine the allowed redshift evolution in either the normalization or slope of the $M_{\text{BH}}-\sigma$ relation consistent with constraints from the observed $M_{\text{BH}}-\sigma$ relation at $z = 0$, under the assumption that black holes of mass M_{BH} form at a characteristic epoch z_f . The redshift evolution of the normalization in our simulations yields a dispersion in the $z = 0$ relation consistent with the observed scatter. We further relate our simulations to ongoing efforts to measure the $M_{\text{BH}}-\sigma$ relation in high-redshift AGNs and discuss future observational tests for normal galaxies at high redshifts with the next generation of large-aperture telescopes.

We describe our simulation methodology in § 2, report our results in § 3, compare with observational constraints in § 4, discuss our results in § 5, and summarize and conclude in § 6. For our cosmological parameters, we adopt a flat universe with $\Omega_m = 0.3$, $\Omega_\Lambda = 0.7$, $\Omega_b = 0.04$, and $h = 0.7$.

2. METHODOLOGY

We have performed a set of 112 simulations of merging galaxies using the entropy-conserving formulation (Springel & Hernquist 2002) of smoothed particle hydrodynamics (SPH; Lucy 1977; Gingold & Monaghan 1977), as implemented in the GADGET code (Springel et al. 2001; Springel 2006). Each progenitor galaxy is constructed using the method described by Springel et al. (2005b), generalized to allow for the expected redshift scaling of galaxy properties. For a progenitor with virial velocity V_{vir} at redshift z we determine a virial mass and radius, assuming a virial overdensity $\Delta_{\text{vir}} = 200$ times the critical density, using the relations

$$M_{\text{vir}} = \frac{V_{\text{vir}}^3}{10GH(z)}, \quad (1)$$

$$R_{\text{vir}} = \frac{V_{\text{vir}}}{10GH(z)}. \quad (2)$$

For the Navarro-Frenk-White concentration (Navarro et al. 1997) of each progenitor dark matter halo, we follow Bullock et al. (2001) and adopt

$$C_{\text{vir}} \simeq 9 \left[\frac{M_{\text{vir}}}{M_\star(z=0)} \right]^{-0.13} (1+z)^{-1}, \quad (3)$$

where $M_\star(z=0) \sim 8 \times 10^{12} h^{-1} M_\odot$ is the linear collapse mass at the present epoch, and $H(z)$ is the Hubble parameter. The concentration and virial radius are then used to create Hernquist (1990) profile dark matter halos using the conversion described by Springel et al. (2005b). The halos are populated with exponential disks of mass $M_{\text{disk}} = 0.041M_{\text{vir}}$ and fractional gas content f_{gas} , whose scale lengths R_d are determined using the Mo et al. (1998) formalism, assuming the specific angular momentum

TABLE 1
MERGER PROGENITOR MODELS

Models	Progenitor V_{vir} (km s^{-1})	Redshift	Gas Fraction (f_{gas})	ISM Pressurization (q_{EOS})	Thermal Coupling (η_{therm})
Local.....	80, 115, 160, 226, 320, 500	$z = 0$	0.4, 0.8	0.25, 1.0	0.05
Intermediate z	80, 115, 160, 226, 320, 500	$z = 2, 3$	0.4, 0.8	0.25, 1.0	0.05
High z	115, 160, 226, 320, 500	$z = 6$	0.4, 0.8	0.25, 1.0	0.05
Low η_{therm}	115, 160, 226, 320, 500	$z = 6$	0.4, 0.8	0.25, 1.0	0.025

content j_d equals the disk mass fraction m_d and a constant halo spin $\lambda = 0.033$. The distribution of halo spins in dissipationless simulations is measured to be independent of mass and redshift (Vitvitska et al. 2002), and our chosen value for λ is near the mode of the distribution. The vertical scale heights of the stellar disks are set to $0.2R_d$, similar to the Milky Way scaling (Siegel et al. 2002). The vertical scale heights of the gaseous disks are determined via an integral constraint on the surface mass density, a self-consistent determination of the galaxy potential, and the effective EOS of the multiphase interstellar medium (ISM; McKee & Ostriker 1977; Springel & Hernquist 2003). The model for the ISM used in these simulations accounts for the multiphase nature of star-forming gas in galaxies by volume averaging the mass-weighted thermodynamic properties of cold clouds and a hot, diffuse component on scales not numerically resolved. Springel & Hernquist (2003) presented a detailed discussion of the implementation and implications of this treatment of the ISM, but the primary dynamical effect of this multiphase model is to pressurize the ISM as the hot, diffuse component increases the effective temperature of the star-forming gas. The effective EOS of the gas (for a numerical fit, see Robertson et al. 2004) therefore acts to stabilize dense gas in galactic disks against Toomre (1964) instabilities caused by self-gravitation (Springel & Hernquist 2003; Robertson et al. 2004; Springel et al. 2005b). The pressurization of the ISM can be varied using an EOS softening parameter, q_{EOS} (for details, see Springel et al. 2005b), which linearly interpolates between isothermal gas ($q_{\text{EOS}} = 0$) and a strongly pressurized multiphase ISM ($q_{\text{EOS}} = 1$).

Each initial galaxy model consists of 40,000 gas particles, 60,000 dark matter particles, and 40,000 stellar particles. The gravitational softening of gas and stellar particles is set to $100 h^{-1}(1+z)^{-1}$ pc. The progenitors merge on prograde-parabolic orbits, with an initial separation $R_{\text{init}} = 5R_{\text{vir}}/8$ and pericentric distance $R_{\text{peri}} = 2R_d$. Each progenitor galaxy contains a “sink” particle with a black hole seed of mass $10^5 h^{-1} M_{\odot}$ allowed to grow through a model based on Bondi-Hoyle-Lyttleton accretion (Hoyle & Lyttleton 1939; Bondi & Hoyle 1944; Bondi 1952), implemented as a subresolution numerical model by Springel et al. (2005b). The Bondi accretion rate onto the black hole is determined by the surrounding gas properties. To allow for black hole growth, the black hole particle is allowed to probabilistically accrete gas particles, but as explained in Springel et al. (2005b) this accreted gas is added to a reservoir from which the Bondi rate is smoothly calculated. The black hole particles typically accrete ~ 100 SPH particles during the evolution of the simulations, depending on the details of the galaxy models and mergers. In this model, a fraction $\epsilon_r = 0.1$ of the mass accretion rate $\dot{M}c^2$ is radiated, and a fraction $\eta_{\text{therm}} = 0.05$ of this 10% is deposited as thermal feedback into the surrounding gas in a kernel-weighted manner. The thermal coupling is calibrated to reproduce the normalization of the local $M_{\text{BH}}-\sigma$ relation (Di Matteo et al. 2005), and we note that other prescriptions for the energy deposition from black hole feedback can produce similar $M_{\text{BH}}-\sigma$

scalings (e.g., Murray et al. 2005). We therefore expect our results to be somewhat insensitive to the exact choice for how the feedback energy couples to the gas, as long as the energy is deposited near the black hole. As our intent is to calculate the development of the $M_{\text{BH}}-\sigma$ relation over time and to avoid assumptions about the presence or form of the $M_{\text{BH}}-\sigma$ relation at higher redshifts, the progenitor models do not contain bulges, but instead yield an $M_{\text{BH}}-\sigma$ relation self-consistently through the merger process.

We simulate equal-mass mergers of progenitors appropriate for redshifts $z = 0, 2, 3$, and 6, with virial velocities in the range $V_{\text{vir}} = 80-500 \text{ km s}^{-1}$. For each virial velocity, progenitors with gas fractions $f_{\text{gas}} = 0.4, 0.8$ and EOS softenings $q_{\text{EOS}} = 0.25, 1.0$ are simulated. The $z = 6$ runs are also repeated using a thermal coupling constant of $\eta_{\text{therm}} = 0.025$ to gauge the effect of altering the efficiency with which black hole feedback heats the surrounding ISM. Table 1 summarizes our full set of simulations. The current set of simulations concerns the $M_{\text{BH}}-\sigma$ relation generated during the primary growth phase of the SMBH, which likely requires a major merger to drive the massive inflow of gas to the centralmost regions of the colliding galaxies. Future calculations of possible evolution in the $M_{\text{BH}}-\sigma$ relation should ideally involve cosmological simulations of galaxy formation that naturally account for the mass spectrum of merger progenitors. Although such simulations are still in development, we note that very minor mergers have been shown to produce only weak star formation in the more massive progenitor for even gas-rich systems as the feeble tidal torquing fails to produce strong disk instabilities in the merging galaxies (T. J. Cox et al. 2006, in preparation). The ability of the most minor mergers to affect a change in the $M_{\text{BH}}-\sigma$ relation in the more massive progenitor galaxies should also be limited.

After the completion of a merger, the projected half-mass effective radius R_e and the mass-weighted line-of-sight stellar velocity dispersion σ measured within an aperture of radius R_e are calculated for each remnant galaxy for many viewing angles. This determination of σ for simulated systems is commensurate with the observational method of Gebhardt et al. (2000) that measures a luminosity-weighted velocity dispersion within an effective radius. The black hole mass M_{BH} in each galaxy is tracked during the simulation and compared with the average dispersion σ to examine any resulting $M_{\text{BH}}-\sigma$ correlation.

3. RESULTS

Figure 1 shows the $M_{\text{BH}}-\sigma$ relation produced by the merging of progenitor galaxies appropriate for redshifts $z = 0, 2, 3$, and 6 (*top left to bottom right*). At each redshift, we perform a least-squares fit to the $M_{\text{BH}}-\sigma$ relation of the form

$$\log M_{\text{BH}} = \alpha + \beta \log(\sigma/\sigma_0), \quad (4)$$

where the relation is defined relative to $\sigma_0 = 200 \text{ km s}^{-1}$. The observed relation has a normalization coefficient $\alpha = 8.13$ and

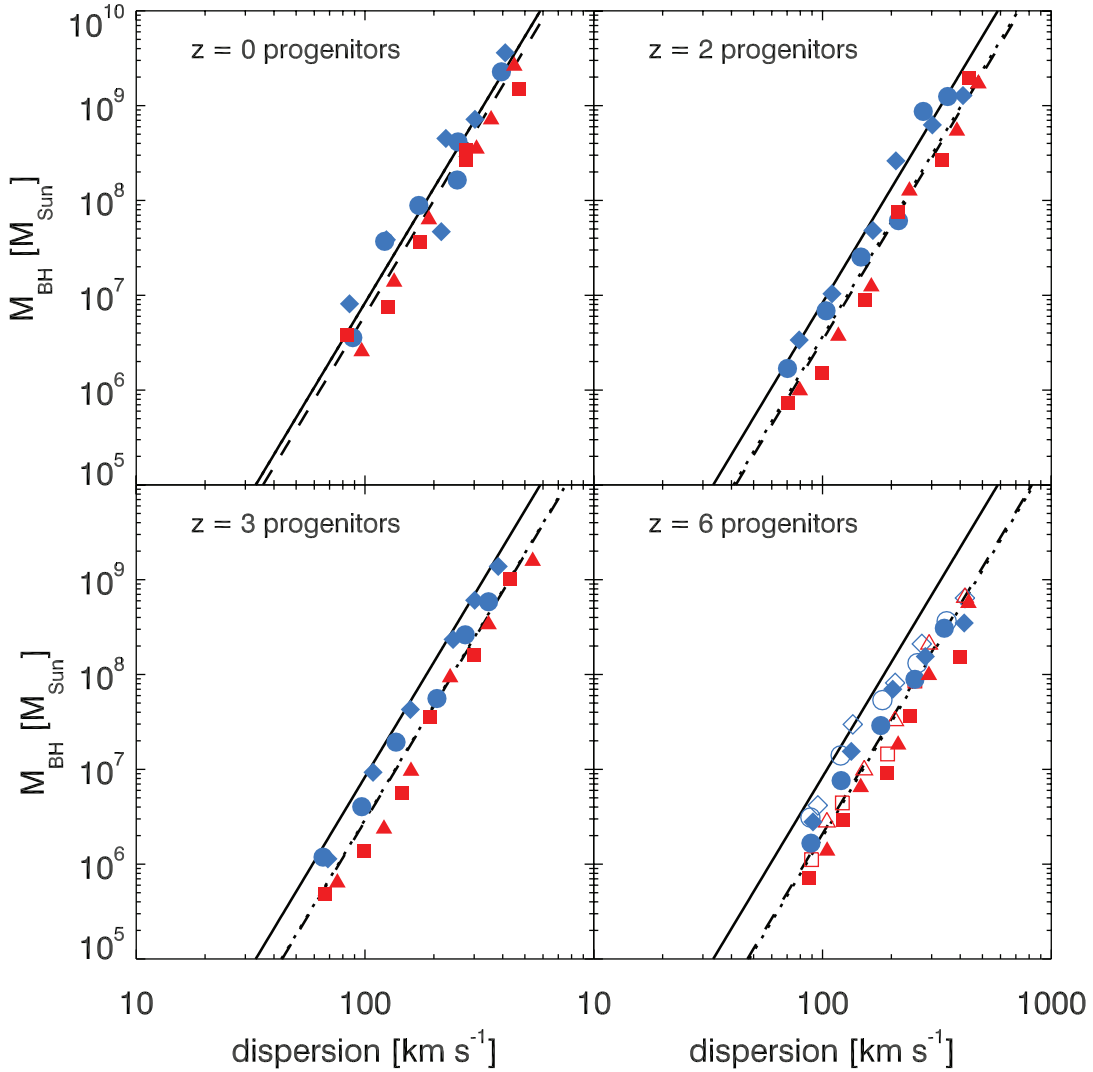


FIG. 1.—Relation between black hole mass M_{BH} and stellar velocity dispersion σ produced by the merging of disk galaxy progenitors appropriate for redshift $z = 0, 2, 3,$ and 6 . These disk mergers produce nearly the same $M_{\text{BH}}-\sigma$ scaling at all redshifts considered, while the simulated relations display a weak redshift evolution in their normalization. For normalization evolution of the form $\sigma \sim \sigma_{z=0}(1+z)^\xi$, the normalization experiences a redshift scaling in the range $\xi = 0.138$ (relative to the simulated $z = 0$ normalization; *dashed lines*) to $\xi = 0.186$ (relative to the observed $z = 0$ normalization; *dotted lines*). At each redshift, we vary the gas fraction f_g and the pressurization of the interstellar medium q_{EOS} (see Springel et al. 2005a), and we plot results for M_{BH} and σ in progenitor models with $g_f = 0.4, q_{\text{EOS}} = 0.25$ (blue circles); $g_f = 0.8, q_{\text{EOS}} = 0.25$ (blue diamonds); $g_f = 0.4, q_{\text{EOS}} = 1.0$ (red squares); and $g_f = 0.8, q_{\text{EOS}} = 1.0$ (red triangles). The T02 best fit to the local $M_{\text{BH}}-\sigma$ relation (black line) is plotted for reference. Also shown is the $M_{\text{BH}}-\sigma$ relation for $z = 6$ progenitors calculated assuming a decreased thermal coupling for black hole feedback (open symbols). Lowering the thermal coupling for black hole feedback by half results in only a small increase in the final black hole mass.

slope $\beta = 4.02$ (T02; Fig. 1, *solid line*). Table 2 lists the best-fit α and β from the simulations at each redshift, along with the dispersion $\Delta_{\log M_{\text{BH}}}$ about each best-fit relation. Table 2 also reports the best-fit normalization $\alpha^{\beta=4.02}$ and resultant dispersion $\Delta_{\log M_{\text{BH}}}^{\beta=4.02}$, assuming the slope of the $M_{\text{BH}}-\sigma$ relation is a constant $\beta = 4.02$ with redshift. The intrinsic $M_{\text{BH}}-\sigma$ dispersion at any given redshift induced by varying the gas fraction or ISM EOS is

TABLE 2
BEST-FIT $M_{\text{BH}}-\sigma$ RELATIONS

Progenitor Redshift	α	β	$\Delta_{\log M_{\text{BH}}}$	$\alpha^{\beta=4.02}$	$\Delta_{\log M_{\text{BH}}}^{\beta=4.02}$
$z = 0$	8.01	3.87	0.26	8.01	0.26
$z = 2$	7.83	4.10	0.28	7.83	0.28
$z = 3$	7.72	4.02	0.26	7.72	0.26
$z = 6$	7.44	3.62	0.24	7.45	0.26

similar to the observed dispersion $\Delta_{\log M_{\text{BH}}} = 0.25-0.3$ (T02). As Figure 1 and Table 2 demonstrate, an $M_{\text{BH}}-\sigma$ relation consistent with a power-law scaling of index $\beta \simeq 4$ is predicted by our modeling for normal galaxies out to high redshift. We infer that the physics that sets the scaling of the $M_{\text{BH}}-\sigma$ relation is insensitive to an extremely wide range of galaxy properties. Virial velocities of the progenitors range from $V_{\text{vir}} = 80$ to 500 km s^{-1} at each redshift, while the dark matter concentrations range from $C_{\text{vir}} \simeq 15.6$ in the smallest progenitor at $z = 0$ to $C_{\text{vir}} \simeq 1.5$ in the largest progenitor at $z = 6$. For the $M_{\text{BH}}-\sigma$ relation at each redshift, models with moderate ISM pressurization typically experience slightly more black hole growth than models with strong ISM pressurization. The increased thermal feedback in the model with a stiffer EOS improves the dynamical stability of the gas, lessens gas angular momentum loss during the merger (Robertson et al. 2004, 2006), and results in less fueling of the black hole (H06a).

3.1. The Normalization of the $M_{\text{BH}}\text{-}\sigma$ Relation with Redshift

The normalization of the $M_{\text{BH}}\text{-}\sigma$ relation evolves weakly with redshift, relative to the observed $z = 0$ result. To characterize this, we generalize the parameterization of the $M_{\text{BH}}\text{-}\sigma$ relation to the form

$$\log M_{\text{BH}} = \alpha + \beta \log\left(\frac{\sigma}{\sigma_0}\right) - \xi \log(1+z), \quad (5)$$

with ξ defined to be positive if the characteristic black hole mass decreases with redshift or the characteristic velocity dispersion increases with redshift. We determine the value of ξ for our simulations, assuming either the observed $z = 0$ normalization $\alpha_{\text{obs}} = 8.13$ (Fig. 1, *dotted lines*) or the calculated $z = 0$ normalization $\alpha_{\text{calc}} = 8.01$ (Fig. 1, *dashed lines*) with the slope fixed at $\beta = 4.02$. We find evidence for a weak evolution, with $\xi = 0.186$ for α_{obs} and $\xi = 0.138$ for α_{calc} using the best-fit parameters reported in Table 2. We now consider whether the weak evolution we find in the normalization of the $M_{\text{BH}}\text{-}\sigma$ relation represents a physical effect caused by the redshift-dependent properties of the progenitors or is an artifact of our modeling.

3.1.1. Systematic Considerations

The systematic effects of our modeling include the redshift scaling of halo virial properties and an assumed fixed thermal coupling of black hole feedback to the gas in our simulations. The form of the progenitor galaxies is inferred from the linear theory of dissipational galaxy formation and is therefore idealized, but in the absence of cosmological simulations with comparable resolution that include feedback from SMBH growth, our choice appears well motivated. While the model considered here assumes a fixed thermal coupling for black hole feedback, if the thermal coupling changes with some bulk property of galaxies with redshift (e.g., metallicity), then this assumption may influence our results. The magnitude of thermal coupling $\eta_{\text{therm}} = 0.05$ of black hole feedback to the surrounding gas is calibrated to reproduce the locally observed relation. To illustrate the impact of this choice, Figure 1 shows the change in normalization of the $M_{\text{BH}}\text{-}\sigma$ relation for $z = 6$ progenitors introduced by lowering the thermal coupling parameter to $\eta_{\text{therm}} = 0.025$ (Fig. 1, *bottom right, open symbols*). As the coupling of the feedback to the gas of the galaxy is decreased, the rate of energy input to the surrounding material by a black hole of a given mass and accretion rate is lessened. The transition between Eddington-limited and self-regulated growth then occurs at a correspondingly higher black hole mass and, as a result, the final mass of the SMBH increases. Decreasing the thermal coupling also mildly flattens the slope of the relation for the highest mass black holes. Overall, the change in the thermal coupling does not renormalize the $M_{\text{BH}}\text{-}\sigma$ relation for $z = 6$ progenitors to coincide with the T02 result. We also note that varying the gas fraction in the progenitors from $f_{\text{gas}} = 0.4$ to 0.8 has little effect on either the normalization or the scaling of the relation at any given redshift.

A sensible measure to gauge a possible evolution of the black hole growth with redshift is the comparison of black hole mass M_{BH} with total stellar mass M_* , which serves as a convenient proxy for the observed $M_{\text{BH}}\text{-}M_{\text{bulge}}$ relation. Figure 2 shows the $M_{\text{BH}}\text{-}M_*$ relation for mergers at all redshifts we consider, with the Marconi & Hunt (2003; Fig. 2, *solid line*) and Magorrian et al. (1998; Fig. 2, *dotted line*) $M_{\text{BH}}\text{-}M_{\text{bulge}}$ relations plotted for comparison. We show the largest stellar mass systems, which are mostly spheroidal and lie near the Marconi & Hunt (2003) relation. Any redshift-dependent impact on the black hole mass at a given stellar mass is not discernibly stronger than the black

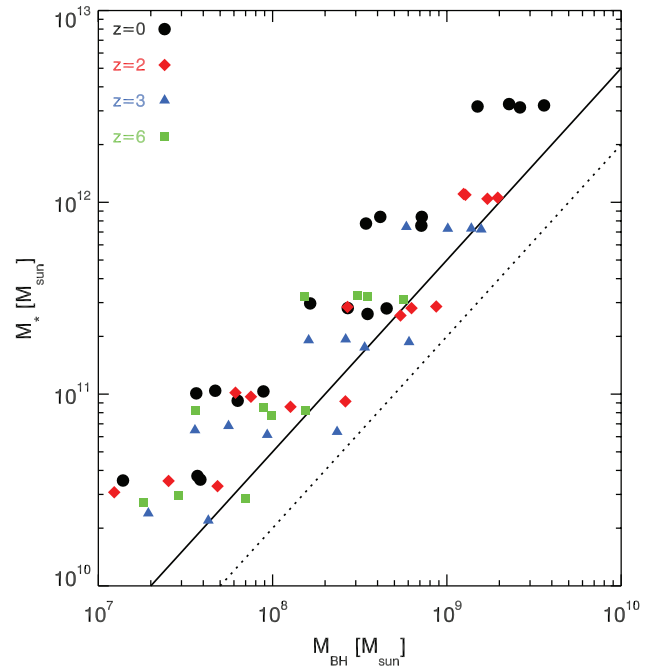


FIG. 2.—Relation between total stellar mass M_* and black hole mass M_{BH} for merger progenitors appropriate for redshifts $z = 0$ (black circles), $z = 2$ (red diamonds), $z = 3$ (blue triangles), and $z = 6$ (green squares). The ratio of black hole to stellar mass remains roughly constant for progenitors at all redshifts we consider, indicating that the normalization evolution of the $M_{\text{BH}}\text{-}\sigma$ relation measured in the simulations is *not* due to a decoupling of bulge and black hole growth. At each circular velocity and redshift, four models for the gas fraction and interstellar medium EOS are considered. We plot bulge-dominated remnants only. The $M_{\text{BH}}\text{-}M_{\text{bulge}}$ relations observed by Marconi & Hunt (2003; *solid line*) and Magorrian et al. (1998; *dotted line*) are shown for comparison.

hole mass increase for decreasing ISM pressurization and increasing gas fraction. We therefore conclude that the systematic uncertainties of our modeling do not generate an unphysical evolution in the black hole mass. Instead, it appears more likely that the variation of the normalization of the $M_{\text{BH}}\text{-}\sigma$ relation with redshift has a physical origin in the structural changes of the merging galaxies, a possibility we examine next.

3.1.2. Physical Considerations

The redshift-dependent structure of progenitor systems expected from the cosmological scalings of galaxy properties provides a plausible explanation for the weak evolution in the normalization of the $M_{\text{BH}}\text{-}\sigma$ relation with redshift. For example, the depth of the potential well in the center of each remnant will influence the velocity dispersion, while for the regions where the baryons dominate, the stellar mass of the spheroid determines the potential. The characteristic densities of the progenitors and remnants increase with redshift, and any relation involving the stellar mass may evolve cosmologically. Similar trends can be measured with our simulations. Figure 3 shows the stellar velocity dispersion as a function of the total stellar mass of each remnant for the simulations at each redshift, along with a stellar mass formulation of the Faber-Jackson luminosity–stellar velocity dispersion relation found from the combination of the Marconi & Hunt (2003) $M_{\text{BH}}\text{-}M_{\text{bulge}}$ and T02 $M_{\text{BH}}\text{-}\sigma$ relations (Fig. 3, *solid line*). For a given stellar mass, the velocity dispersion increases for higher redshift progenitors, with the greatest increase for the most spheroid-dominated systems. We therefore ascribe the weak evolution in the normalization of the $M_{\text{BH}}\text{-}\sigma$ relation with redshift to a systematically increasing σ for a given M_{BH} or M_* and argue

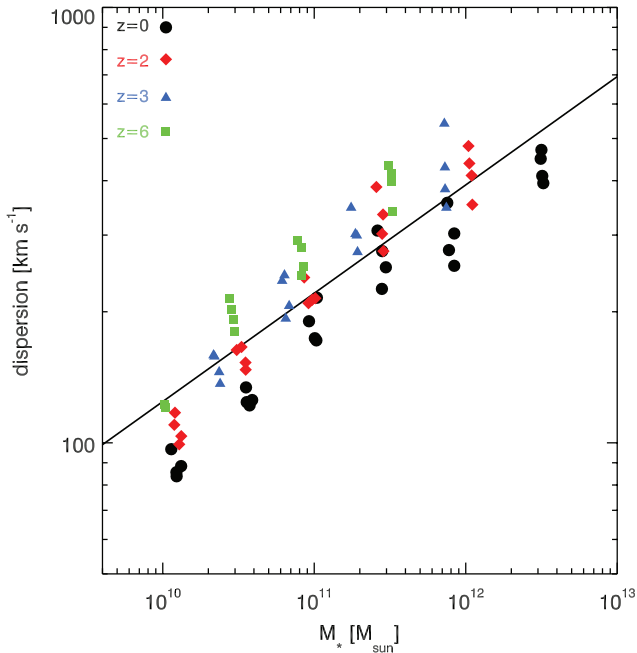


FIG. 3.—Relation between stellar velocity dispersion σ and total stellar mass M_* of remnants for merger progenitors appropriate for redshifts $z = 0$ (black circles), $z = 2$ (red diamonds), $z = 3$ (blue triangles), and $z = 6$ (green squares). The simulated remnants display an increasing velocity dispersion for a given stellar mass with redshift, which may be viewed as a weak evolution in the Faber & Jackson (1976) relation. The evolution in velocity dispersion for a given stellar mass induces a corresponding evolution in the calculated $M_{\text{BH}}-\sigma$ relation (see Fig. 1). At each circular velocity and redshift, four models for the gas fraction and interstellar medium EOS are considered. A total stellar mass version of the Faber-Jackson relation constructed by combining the T02 $M_{\text{BH}}-\sigma$ and Marconi & Hunt (2003) $M_{\text{BH}}-M_{\text{bulge}}$ relations is shown for comparison (solid line).

that the steeper potential wells of high-redshift galaxies are a primary cause for this apparent redshift evolution in the stellar mass formulation of the Faber-Jackson relation.

The evolution of the stellar velocity dispersion for a given stellar mass between redshifts $z = 2$ and 6 can be compared with the redshift-dependent properties of our progenitor models. Changes in the structure of galaxies can lead to an evolution in the stellar velocity dispersion that scales with redshift in a similar fashion to the evolving normalization in our calculated $M_{\text{BH}}-\sigma$ relations at redshifts $z = 2-6$. A possible origin for these effects can be illustrated by the use of a simple galaxy model that demonstrates the impact of redshift-dependent structural properties on the central stellar kinematics. To demonstrate this, we consider the velocity dispersion of a stellar spheroid residing within a dark matter halo with fixed virial mass M_{vir} as a function of redshift. For simplicity, we assume that the stellar mass within the halo is a fixed fraction of the virial mass and that the central potential is dominated by the baryons. We model both the dark matter halo and stellar spheroid as Hernquist profiles, with the stellar spheroid scale length a_s a fraction b of the halo scale length a_h . Equations (1)–(3) describe the redshift scalings of the dark matter halos for a given virial velocity V_{vir} . Incorporating the results from Springel et al. (2005b), we find that the spheroid scale length depends on the virial mass and redshift as

$$a_s(M_{\text{vir}}, z) = \frac{b}{C_{\text{vir}}} \sqrt{2 \left[\ln(1 + C_{\text{vir}}) - \frac{C_{\text{vir}}}{(1 + C_{\text{vir}})} \right]} \times (GM_{\text{vir}})^{1/3} [10H(z)]^{-2/3}, \quad (6)$$

where C_{vir} is the mass- and redshift-dependent concentration given by equation (3). The stellar velocity dispersion of the Hernquist profile depends on the scale length as $\sigma \propto a_s^{-1/2}$. The power-law scaling of $\sigma \propto (1+z)^\xi$ for $2 < z < 6$ then ranges from $\xi \approx 0.17$ for a $M_{\text{vir}} \sim 10^{10} M_\odot$ halo to $\xi \approx 0.28$ for $M_{\text{vir}} \sim 10^{14} M_\odot$, which encompasses the approximate scaling ξ found in the simulations. Below redshift $z = 2$, the redshift evolution of the stellar velocity dispersion begins to flatten and is roughly constant between redshifts $z = 0$ and 1. The relative constancy of the stellar velocity dispersion in this redshift regime is caused by the growing influence of the cosmological constant on the Hubble parameter, as it balances the increase in the virial concentration. We therefore expect the normalization of the $M_{\text{BH}}-\sigma$ relation to remain roughly fixed for purely dissipationless systems between $z = 0$ and 1 and to begin to evolve roughly as a weak power law in $1+z$ toward higher redshifts. For the dissipational systems we simulate, an additional increase in the stellar velocity dispersion between redshifts $z = 0$ and 2 beyond the estimate for purely stellar systems is needed to fully explain the evolution measured in the simulations by redshift $z = 2$. We leave such an exploration for future work but note here that either gas dissipation or feedback effects from the SMBH may influence the scaling of the stellar dispersion with redshift or its mass dependence.

4. COMPARISON WITH OBSERVATIONS

4.1. Scatter Induced in the Local $M_{\text{BH}}-\sigma$ Relation by Redshift Evolution

If the $M_{\text{BH}}-\sigma$ relation evolves with redshift, any redshift evolution in the cosmic black hole population will affect the statistical distribution of galaxies about the observed $M_{\text{BH}}-\sigma$ relation at $z = 0$. Following the formalism presented by Yu & Lu (2004, hereafter YL04), we can statistically characterize the connection between AGNs and the local $M_{\text{BH}}-\sigma$ relation by assuming that black hole growth occurs primarily during periods of quasar activity. If we further assume that the $M_{\text{BH}}-\sigma$ relation generated by mergers at each redshift has an intrinsically small scatter, we can calculate the allowed redshift evolution in σ given M_{BH} consistent with the dispersion measured in the local $M_{\text{BH}}-\sigma$ relation.

From $P(z_f | \log M_{\text{BH}})$, the probability distribution function (PDF) for a black hole of mass M_{BH} to have formed at a redshift z_f , we can calculate the expectation value of a function $q(z_f, \log M_{\text{BH}})$, given $\log M_{\text{BH}}$, as

$$\langle q | \log M_{\text{BH}} \rangle = \int q(z_f, \log M_{\text{BH}}) P(z_f | \log M_{\text{BH}}) dz_f, \quad (7)$$

and the moments about $\langle q | \log M_{\text{BH}} \rangle$ as

$$\mu_n^q = \int [q(z_f, \log M_{\text{BH}}) - \langle q | \log M_{\text{BH}} \rangle]^n P(z_f | \log M_{\text{BH}}) dz_f. \quad (8)$$

We can identify the expectation value $\langle \sigma | \log M_{\text{BH}} \rangle$ with the $M_{\text{BH}}-\sigma$ relation observed at $z = 0$ and associate the second moment with the measured $M_{\text{BH}}-\sigma$ relation dispersion $\Delta_{\log M_{\text{BH}}}^{\text{obs}} \equiv (\mu_2^\sigma)^{1/2} = 0.25-0.3$ dex (T02). If the velocity dispersion depends on some larger set of independent variables \bar{x} as $\sigma(\log M_{\text{BH}}, \bar{x})$, and $P(z_f | \log M_{\text{BH}})$ is independent of \bar{x} , we can extend this definition of the expectation value to calculate, e.g., $\langle \sigma | \log M_{\text{BH}}, \bar{x} \rangle$. The analysis of YL04 treats a more general scenario in which joint PDFs for properties associated with black hole mass are functions of more than one variable, and we restrict our attention to a single PDF directly relating z_f and $\log M_{\text{BH}}$. Equivalently, that

$P(z_f | \log M_{\text{BH}})$ is independent of \bar{x} reflects our operating assumptions, including (1) all scatter in the $M_{\text{BH}}-\sigma$ at $z = 0$ is due to evolution in σ with redshift (i.e., if \bar{x} is null, σ does not depend on z , and the dispersion in the $M_{\text{BH}}-\sigma$ relation would be $\Delta_{\log M_{\text{BH}}} = 0$), and (2) galactic evolution subsequent to the primary growth phase of the black hole does not affect the direct connection between z_f and $\log M_{\text{BH}}$.

The $M_{\text{BH}}-\sigma$ relation generated by the merging of progenitor galaxies appropriate for a range of redshifts demonstrates an evolution in its normalization with respect to the observed relation at $z = 0$. By using a known $P(z_f | \log M_{\text{BH}})$ and a functional form for $\sigma(z, \log M_{\text{BH}}, \bar{x})$ that captures this evolution, the dispersion about the average relation $\langle \sigma | \log M_{\text{BH}}, \bar{x} \rangle$ can be calculated and compared with the observed $\Delta_{\log M_{\text{BH}}}^{\text{obs}}$. The small observed scatter in the $M_{\text{BH}}-\sigma$ relation will then constrain \bar{x} for a known $P(z_f | \log M_{\text{BH}})$. To this end, we consider $M_{\text{BH}}-\sigma$ relations with an evolution in normalization of the form of equation (5), with the identification of $\bar{x} = \xi$, or an evolution in the slope of the form

$$\log M_{\text{BH}} = \alpha + \beta(1+z)^\phi \log\left(\frac{\sigma}{\sigma_0}\right), \quad (9)$$

with $\bar{x} = \phi$. We proceed to calculate the resulting variance μ_2^σ about the mean $M_{\text{BH}}-\sigma$ relation at $z = 0$, using these forms for $\sigma(M_{\text{BH}}, z)$ and the observed values of $\alpha = 4.0$ and $\beta = 8.13$ (T02). As the sign of either ϕ or ξ will strongly affect the symmetry of the inferred distribution about the mean relation, we also characterize the skewness $\gamma_1 = \mu_3^\sigma / (\mu_2^\sigma)^{3/2}$.

We now adopt a form for $P(z_f | \log M_{\text{BH}})$, using the results of H06a, and calculate the probability $P(z_f | \log M_{\text{BH}})$ for a black hole of mass M_{BH} to have formed at redshift z_f . The H06a modeling uses luminosity-dependent quasar lifetimes and obscuring column density distributions measured from the simulations presented in this paper to infer the black hole mass function $n(M_{\text{BH}}, z)$ from a host of constraints from observations of quasars. The evolution of $n(M_{\text{BH}}, z)$ with redshift is primarily determined by an evolving characteristic luminosity, $L_*(z)$, that determines the location of the maximum of $n[M_{\text{BH}}(L), z]$. In principle, $P(z_f | \log M_{\text{BH}})$ is well determined in the context of the H06a model for the cosmic black hole population via the observed evolution of quasar luminosity functions in multiple wavebands and constraints on the mass density of black holes at $z = 0$. In practice, the somewhat weak observational constraint on the evolution of the break in the luminosity function at the highest observationally accessible redshifts requires a choice for the functional form of the evolving characteristic luminosity $L_*(z)$, which determines the peak of the black hole mass function $n[M_{\text{BH}}(L), z]$. As an *Ansatz* we adopt the form for $L_*(z)$ chosen by H06a to best fit the available constraints from observations, although we note that the calculations presented in § 6 of H06a, and below, can be applied to more general forms of $n(M_{\text{BH}}, z)$ and $L_*(z)$, and the analysis presented here could be repeated for interpretations of the quasar luminosity function other than that adopted by H06a.

The resulting $P(z_f | \log M_{\text{BH}})$, plotted in an integral form in Figure 4 and reproduced from H06a, reflects the best-fit model for the evolution of the cosmic black hole population given the available data and the H06a interpretation of the quasar luminosity function. Cosmic downsizing, the concept that black holes of larger mass formed characteristically at higher redshifts (e.g., Cowie et al. 2003; Steffen et al. 2003), is apparent in our $P(z_f | \log M_{\text{BH}})$, as the formation-redshift PDF for low-mass black holes increases strongly at low redshifts. The characteristic downsizing of black hole masses as the universe ages leads to an immediate general conclusion about possible evolution in the $M_{\text{BH}}-\sigma$

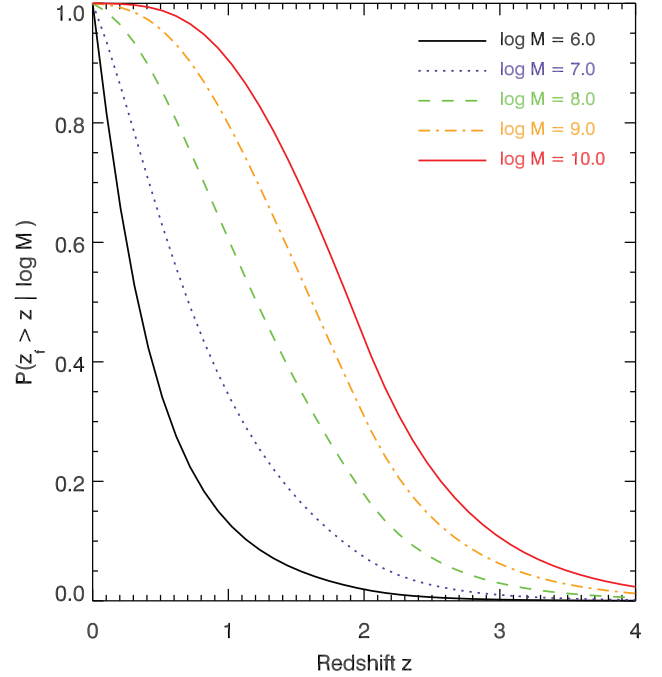


FIG. 4.—Integrated probability distribution function $P(z_f > z | \log M_{\text{BH}})$ for a SMBH of mass M_{BH} to have formed at a redshift $z_f > z$, as determined by the best-fit model of H06a (see § 4.1 for details). Shown is the $P(z_f > z | \log M_{\text{BH}})$ for $\log M_{\text{BH}} = 6.0$ (black line), 7.0 (purple line), 8.0 (blue line), 9.0 (green line), and 10.0 (red line). More massive black holes are typically formed at successively higher redshifts, reflecting the cosmic downsizing trend inferred from evolution in the quasar luminosity function. This $P(z_f > z | \log M_{\text{BH}})$ distribution is combined with functional forms for redshift-dependent $M_{\text{BH}}-\sigma$ relations to estimate constraints on possible evolution in the $M_{\text{BH}}-\sigma$ relation by comparing with observations at $z = 0$ (see Figs. 5 and 6).

relation: if black holes of differing masses form at different characteristic redshifts, any evolution in the $M_{\text{BH}}-\sigma$ relation will introduce an M_{BH} -dependent dispersion in the observed relation at $z = 0$. While subsequent processes may reduce or amplify the mass dependence of $\Delta_{\log M_{\text{BH}}}$, if observations reveal a trend in $\Delta_{\log M_{\text{BH}}}$ between differing mass bins, the result could be associated with an evolution in the $M_{\text{BH}}-\sigma$ relation. Below, we characterize the mass dependence of the statistical moments of the distribution of galaxies around the mean $M_{\text{BH}}-\sigma$ relation and relate them to possible forms for $M_{\text{BH}}-\sigma$ evolution.

4.1.1. Normalization Evolution

For a normalization evolution of the form of equation (5), the dispersion $\Delta_{\log M_{\text{BH}}}$ and skewness γ_1 for the $M_{\text{BH}}-\sigma$ relation at $z = 0$ can be readily calculated using equations (7)–(8), given a $P(z_f | \log M_{\text{BH}})$ describing the evolution of the cosmic black hole population. Figure 5 shows the dispersion in black hole mass $\Delta_{\log M_{\text{BH}}}$ as a function of SMBH mass introduced in the $M_{\text{BH}}-\sigma$ relation at $z = 0$ by normalization evolution over a range in the power-law index ξ (Fig. 5, left). As $\Delta_{\log M_{\text{BH}}}$ is an even function of ξ , we plot $\Delta_{\log M_{\text{BH}}}$ for different values of $|\xi|$. The observed range of $\Delta_{\log M_{\text{BH}}}^{\text{obs}} = 0.25\text{--}0.3$ dex (Fig. 5, left, red shaded region) can be compared to the normalization evolution measured in the simulations of $\xi \approx 0.138\text{--}0.186$ (Fig. 5, left, blue shaded region), and the simulations agree well with the observational constraints. Given the observational data and our chosen $P(z_f | \log M_{\text{BH}})$, evolution in the normalization with approximately $|\xi| < 0.2$ is allowed. The mass dependence of $\Delta_{\log M_{\text{BH}}}$ directly reflects changes in the black hole population during the evolution of the $M_{\text{BH}}-\sigma$ normalization with redshift, with more massive black holes being

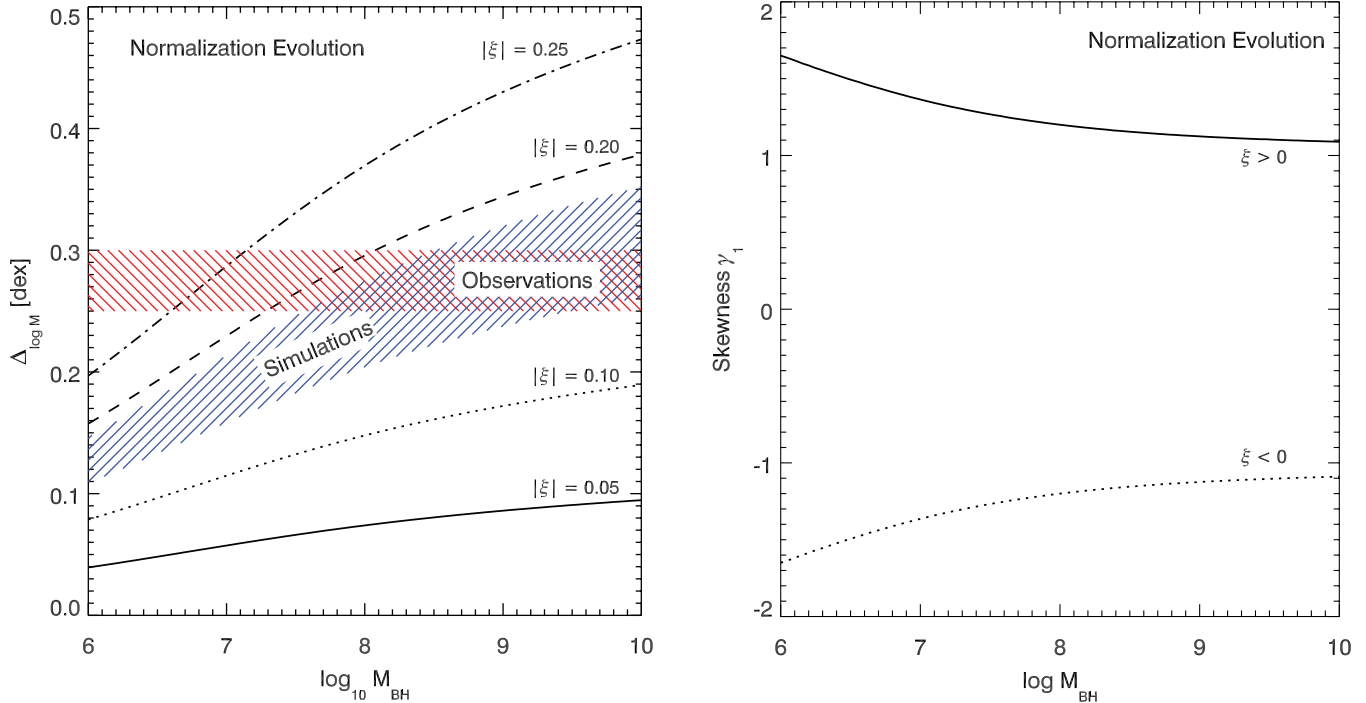


FIG. 5.—Dispersion $\Delta_{\log M_{\text{BH}}}$ (left) and skewness γ_1 (right) about the local $M_{\text{BH}}-\sigma$ relation caused by evolution in the normalization of the $M_{\text{BH}}-\sigma$ relation with redshift of the form $\log(M_{\text{BH}}) = \alpha + \beta \log(\sigma/\sigma_0) - \xi \log(1+z)$. Redshift evolution in the normalization induces a dispersion in the $M_{\text{BH}}-\sigma$ relation at $z=0$, since black holes of different masses form at characteristically different cosmological times (see Fig. 4). The dispersion induced by normalization evolution with redshift scalings of $|\xi| = 0.05$ (solid line), 0.10 (dotted line), 0.20 (dashed line), and 0.25 (dot-dashed line) is plotted. The observed dispersion $\Delta_{\log M_{\text{BH}}}^{\text{obs}} = 0.25-0.3$ (shaded region) provides a tight constraint on the evolution in the normalization, which is limited to approximately $|\xi| < 0.2$. If the normalization evolves, the sign of the skewness in the distribution about the local $M_{\text{BH}}-\sigma$ relation indicates the sign of ξ .

formed during characteristically earlier epochs, when the $M_{\text{BH}}-\sigma$ normalization was more discrepant from the $z=0$ relation than during the formation epoch of SMBHs. As the most massive black holes form over a wider range in redshift than smaller black holes, their broader PDFs also contribute to the scatter about the mean relation. If further sources of scatter in the $M_{\text{BH}}-\sigma$ relation are unimportant, and subsequent galactic evolution does not strongly affect $P(z_f | \log M_{\text{BH}})$, then the slope of $\Delta_{\log M_{\text{BH}}}$ provides direct information about the typical redshift of formation for black holes of a given mass. We note that since the black hole and spheroids form contemporaneously in our model, the evolution owing to ξ in the calculations also suggests a correlation between the deviation of a galaxy from the $M_{\text{BH}}-\sigma$ relation and the age of the spheroidal stellar population. For normalization evolution, such a correlation results from the monotonic mapping of the measured velocity dispersion deviation $\delta_{\log \sigma} \equiv [\log \sigma(M_{\text{BH}}, z_f) - \log \sigma(M_{\text{BH}}, z=0)] = \xi \log(1+z_f)$ to a formation redshift z_f , which means the probability distribution function $P(\delta_{\log \sigma} | \log M_{\text{BH}})$ maps monotonically onto $P(z_f | \log M_{\text{BH}})$.

Further information on ξ can be gleaned from the skewness γ_1 of the distribution (Fig. 5, right). For normalization evolution of the form of equation (5), the resulting skewness has the same sign as the power-law index and immediately indicates whether the $M_{\text{BH}}-\sigma$ normalization increases or decreases with redshift. All positive values of ξ have the same skewness, with the same functional shape as the skewness defined by negative values of ξ reflected about the origin.

4.1.2. Slope Evolution

While our simulated $M_{\text{BH}}-\sigma$ relations do not show any monotonic trend in their slope with redshift, many theories for the $M_{\text{BH}}-\sigma$ relation have some functional dependence in the slope

with redshift or black hole mass (e.g., Sazonov et al. 2005; Wyithe 2006). The dispersion $\Delta_{\log M_{\text{BH}}}$ and skewness γ_1 for the $M_{\text{BH}}-\sigma$ relation owing to slope evolution of the form of equation (9) is also accessible using the method described for characterizing normalization evolution. Figure 6 shows the dispersion $\Delta_{\log M_{\text{BH}}}$ (left) about the local $M_{\text{BH}}-\sigma$ relation induced by slope evolution, plotted for $\phi = 0.2$ (solid line), 0.3 (dashed line), -0.2 (dotted line), and -0.3 (dot-dashed line). To illustrate the mass dependence of $\Delta_{\log M_{\text{BH}}}$ and γ_1 above and below the pivot, we choose the fixed intercept to be $\log M_{\text{BH, fixed}} = \alpha = 8.13$, but the same analysis could be performed for any intercept. For consistency with the observed dispersion $\Delta_{\log M_{\text{BH}}}^{\text{obs}} = 0.25-0.3$ (Fig. 6, left, shaded region), the evolution in the slope is constrained to approximately $|\phi| < 0.3$ for our chosen intercept. If the fixed pivot intercept for a slope evolution of the $M_{\text{BH}}-\sigma$ relation is small ($\log M_{\text{BH}} \approx 6$), then the constraint on $|\phi|$ would be much tighter, as $\Delta_{\log M_{\text{BH}}}$ is a strong function of M_{BH} above the pivot mass. The skewness induced by a slope evolution (Fig. 6, right) contains more information than for normalization evolution. The skewness provides a constraint on the pivot mass if the pivot falls in the observationally accessible range, as the sign of the skewness changes at this intercept in the redshift-dependent relation.

In principle, any model that produces a redshift evolution in the $M_{\text{BH}}-\sigma$ relation can be compared with the observations in a similar manner, and given a $P(z_f | \log M_{\text{BH}})$ for the cosmic black hole population, distinct models for generating the $M_{\text{BH}}-\sigma$ relation could be observationally differentiated. We note here that comparisons with observations are most meaningful if the black holes in the measured $M_{\text{BH}}-\sigma$ relation represent a fair sample of the total black hole population for a given mass bin. For instance, an increase in the number of bulges in spiral systems with well-determined M_{BH} and σ would be helpful. Unfortunately,

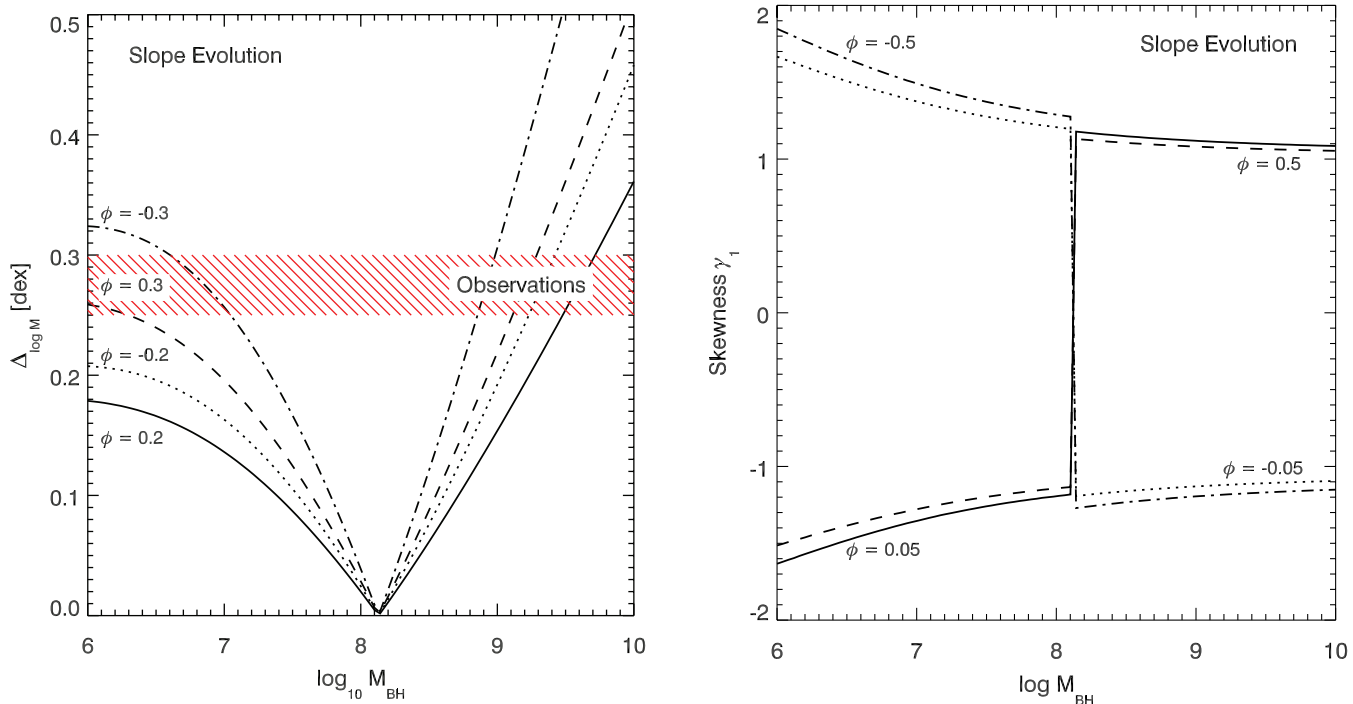


FIG. 6.—Dispersion $\Delta_{\log M_{\text{BH}}}$ (left) and skewness γ_1 (right) about the local $M_{\text{BH}}-\sigma$ relation, induced by an evolution in the slope of the $M_{\text{BH}}-\sigma$ relation with redshift of the form $\log(M_{\text{BH}}) = \alpha + \beta(1+z)^\phi \log(\sigma/\sigma_0)$. Redshift evolution in the slope induces a dispersion in the $M_{\text{BH}}-\sigma$ relation at $z=0$, since black holes of different masses form at characteristically different cosmological times (see Fig. 4). The dispersion is plotted for $\phi = 0.2$ (solid line), 0.3 (dashed line), -0.2 (dotted line), and -0.3 (dot-dashed line). To illustrate the mass dependence of $\Delta_{\log M_{\text{BH}}}$ and γ_1 above and below the pivot, we choose the fixed intercept to be $\log M_{\text{BH, fixed}} = \alpha = 8.13$. The observed dispersion $\Delta_{\log M_{\text{BH}}}^{\text{obs}} = 0.25-0.3$ (shaded region) constrains evolution in the slope to approximately $|\phi| < 0.3$. If the slope of the $M_{\text{BH}}-\sigma$ relation evolves and the intercept falls in the observable range, the sign of ϕ could be constrained by examining the sign of the observed skewness as a function of black hole mass because γ_1 changes sign at the pivot mass.

dust effects make stellar dynamical measurements of late-type galaxies difficult, and a more effective approach for determining black hole masses in these systems will need further development (e.g., Ho et al. 2002). We encourage further observational efforts to eliminate selection biases in the sample used to determine the local $M_{\text{BH}}-\sigma$ relation.

4.2. Observations of $M_{\text{BH}}-\sigma$ in AGNs at $z > 0$

Our simulations can be directly related to the $M_{\text{BH}}-\sigma$ relation in normal galaxies at redshifts $z > 0$. However, previous observational efforts to measure the $M_{\text{BH}}-\sigma$ relation in galaxies beyond the locally accessible sample have concentrated mostly on using the $M_{\text{BH}}-\sigma$ relation indicators in AGNs (Shields et al. 2003; Treu et al. 2004), combining $\text{H}\beta$ line width estimates for black hole mass (e.g., Wandel et al. 1999) and $[\text{O III}]$ line widths as a proxy for stellar velocity dispersion (e.g., Nelson 2000a) or dispersion measurements from stellar spectral features (Treu et al. 2001). Other estimates for the $M_{\text{BH}}-\sigma$ relation in high- z quasars have been made (e.g., Walter et al. 2004) by comparing a black hole mass inferred from Eddington-limited accretion onto a bright quasar with the dynamical mass estimated from Very Large Array (VLA) observations of molecular gas kinematics.

Shields et al. (2003) found that AGNs between $z = 0$ and 3.5 obey an $\text{H}\beta$ - $[\text{O III}]$ relation, consistent with the local $M_{\text{BH}}-\sigma$ relation determined by T02, and the observations at any single redshift were also consistent with the $z = 0$ result, although the statistics are somewhat limited. The observations of Treu et al. (2004) imply a conflicting result with seven AGNs at $z \sim 0.37$ inferred to primarily lie above the $z = 0$ $M_{\text{BH}}-\sigma$ relation, although with significant scatter and large estimated error. The Walter et al. (2004) CO(3-2) observations also place the $z = 6.42$ quasar above the $z = 0$ $M_{\text{BH}}-\sigma$ relation and claim to be inconsistent with

the presence of a stellar bulge of the size needed to match the local $M_{\text{BH}}-M_{\text{bulge}}$ relations.

The increased scatter observed in the AGN samples and the deviation of high- z quasars relative to our calculations may originate in the dynamical state of the observed systems (for a related discussion, see Vestergaard 2004). If these systems correspond to merging galaxies, they may not be dynamically relaxed, and these samples may therefore display a larger range of velocity dispersions than do the dynamically relaxed systems that primarily comprise the locally observed $M_{\text{BH}}-\sigma$ relation or the redshift-dependent $M_{\text{BH}}-\sigma$ relation in relaxed galaxies produced by our simulations. For instance, observations of local Seyfert galaxies show that tidally distorted hosts have systematically higher emission-line widths at a given stellar velocity dispersion (Nelson & Whittle 1996). An exploration of the $M_{\text{BH}}-\sigma$ relation during the peak AGN phases of our simulations is planned in future work, but given the current observational and theoretical uncertainties, we do not believe our simulations are in conflict with the observations. However, our simulations are more consistent with the Shields et al. (2003) claim of no evolution than with either the Treu et al. (2004) or Walter et al. (2004) claims of evidence for evolution in the $M_{\text{BH}}-\sigma$ relation. In our model where the $M_{\text{BH}}-\sigma$ scaling is set during spheroid formation, the evolution of systems tends to occur either quickly in the M_{BH} direction during the exponential growth phase of the black hole or more gradually along the $M_{\text{BH}}-\sigma$ relation during self-regulated black hole growth. The presence of massive black holes at high redshift without massive bulges would be rare in the context of our modeling, and such outliers would likely have to undergo purely stellar major mergers to reach the local $M_{\text{BH}}-\sigma$ relation. We also note that if the Treu et al. (2004) offset of $\delta \log \sigma = -0.16$ measured for AGNs at $z = 0.37$ holds for the $M_{\text{BH}}-\sigma$ relation generated by the merging of

normal galaxies at that redshift, then a power-law evolution in the normalization of σ would imply $\xi = -1.17$. If some subsequent process does not reduce the deviation from the $z = 0$ $M_{\text{BH}}-\sigma$ relation for a given galaxy, then with our $P(z_f|\log M_{\text{BH}})$ and the evolution $\xi = -1.17$ inferred from the Treu et al. (2004) measurements, the scatter in the $M_{\text{BH}}-\sigma$ relation at $z = 0$ would be $\Delta_{\log M_{\text{BH}}} = 0.92-2.215$ over the range $\log M_{\text{BH}} = 6-10$. This scatter is much larger than both the observed dispersion and the dispersion predicted by our simulations and formation redshift distribution $P(z_f|\log M_{\text{BH}})$.

4.3. Observations of Inactive Galaxies at $z > 0$

For the next generation of large telescopes, a measurement of the central stellar velocity dispersion in normal galaxies at high redshifts may be feasible, and our simulations can connect directly with such observations. A proper census of the cosmic black hole population as a function of redshift will necessarily involve an estimate of the mass of SMBHs at the centers of inactive galaxies. Without black hole activity to provide an estimate of the black hole mass, and given the likely prohibitively extreme resolution (< 10 pc) needed for stellar dynamical estimates of SMBH masses, inferring black hole masses through the $M_{\text{BH}}-\sigma$ relation via stellar velocity dispersion measures for the cosmological spheroidal population may provide the best way of constraining the evolution of the black hole population with redshift. These measurements will necessarily involve an assumed model to relate M_{BH} and σ as a function of redshift, such as the relation calculated by our simulations. Our work then provides additional theoretical motivation for attempting these observations with future generations of large infrared-capable telescopes.

Among the large telescopes currently in various stages of development are the Giant Magellan Telescope (GMT, 20–25 m; Johns et al. 2004), California Extremely Large Telescope (CELT, 30 m; Nelson 2000b), Euro50 (50 m; Andersen et al. 2004), Overwhelmingly Large Telescope (OWL, 100 m; Dierickx et al. 2004), Japanese Extremely Large Telescope (30 m; Iye et al. 2004), and Chinese Future Giant Telescope (30 m; Su et al. 2004). The planned capabilities of these telescopes are impressive. For instance, the GMT design calls for a resolution of $\theta_{\text{GLAO}} \approx 0''.15$ with ground-layer adaptive optics (GLAO) and $\theta_{\text{FAO}} \approx 0''.007$ with fully adaptive optics (FAO), corresponding to physical scales at redshift $z = 3$ of $R_{\text{GLAO}} \approx 1.15$ kpc and $R_{\text{FAO}} \approx 54$ pc, respectively. The remnant systems in our simulations appropriate for $z = 3$ progenitors have effective radii ranging from $R_{\text{eff}} \approx 0.3$ to 10 physical kpc, making central stellar velocity dispersion measurements feasible in principle, and likely possible even with GLAO observations for the most massive systems. Infrared spectroscopy of rest-frame UV stellar lines could be used to find central stellar velocity dispersions of spheroids and, combined with the simulation results to estimate M_{BH} via an inversion of the calculated $M_{\text{BH}}-\sigma$ relation for a given redshift, the cosmic black hole population can be constrained (see, e.g., Yu & Tremaine 2002). Future lensing observations with the Square Kilometer Array to measure black hole masses at intermediate redshifts (Rusin et al. 2005) may also be useful in this regard. In addition, if SMBH feedback is important in determining the properties of normal galaxies (e.g., Springel et al. 2005b; Robertson et al. 2006), such observations could prove to be crucial input for theories of galaxy formation during the evolutionary epoch when the most massive black holes are formed.

5. DISCUSSION

Our simulations demonstrate that the merging of disk galaxies whose properties are appropriate for redshifts $z = 0-6$ should

produce an $M_{\text{BH}}-\sigma$ relation with the observed power-law scaling $M_{\text{BH}} \propto \sigma^4$. The $M_{\text{BH}}-\sigma$ relation retains this scaling at redshifts $z = 0-6$, even while the merger progenitors range widely in their structural properties with redshift. A possible weak evolution in the normalization of the $M_{\text{BH}}-\sigma$ relation is found, which may result from an increasing velocity dispersion owing to the redshift evolution of the potential wells of galaxies. Simple arguments for how such evolution would affect the velocity dispersion provide a similar redshift scaling at redshifts $z = 2-6$ to those calculated from the simulations. As these redshift scalings systematically place high-redshift systems below the $z = 0$ $M_{\text{BH}}-\sigma$ relation, subsequent accretion processes may further reduce the scatter in the observed $M_{\text{BH}}-\sigma$ relation over time.

Our results also provide guidance to semianalytical models about the behavior of the $M_{\text{BH}}-\sigma$ relation. We suggest that semianalytical models in the vein of Volonteri et al. (2003) or Menci et al. (2003) could be altered to explicitly maintain the local $M_{\text{BH}}-M_{\text{bulge}}$ relation at redshifts $z < 6$, produce the same $M_{\text{BH}}-\sigma$ scaling at redshifts $z < 6$, and reproduce the local $M_{\text{BH}}-\sigma$ normalization. Simultaneously, such models should tie morphological information, such as spheroidal growth, to the growth of SMBHs (for a related discussion, see Bromley et al. 2004). While some semianalytical models include prescriptions for black hole accretion or feedback (e.g., Menci et al. 2003; Wyithe & Loeb 2003), it is difficult to graft all the effects of feedback onto these models without a detailed treatment of the complex interplay between gas inflows, starbursts, and black hole activity. These models could also be altered to more fully capture the black hole mass-dependent effects of feedback on galaxies and their environments (see also, e.g., H06a).

Overall, our simulations provide more general conclusions about the cosmological evolution of structure. The spheroidal components of galaxies are likely formed in the same process that sets the $M_{\text{BH}}-\sigma$ relation, and therefore the demographics of black holes trace the demographics of spheroids over cosmic time, as is inferred locally (Yu & Tremaine 2002). With the possible shared origin of spheroids and SMBHs in mind, we note that observations suggest that the stellar populations of cluster ellipticals form at redshifts $z > 2$ (e.g., van Dokkum & Stanford 2003; Gebhardt et al. 2003). This era coincides with the epoch $z \sim 3$, during which the most massive SMBHs are formed, as inferred from the evolution in the quasar number density (Schmidt et al. 1995; Boyle et al. 2000). Future comparisons with high-redshift AGNs and massive ellipticals could help provide our modeling of individual mergers with a broader cosmological context. By connecting with the evolution of the observed quasar luminosity function through the $P(z_f|\log M_{\text{BH}})$ supplied by calculations in the vein of H06a, our model may account for cosmological considerations such as evolution in the mass-dependent galaxy merger rate, the cold gas fraction, or the global star formation rate.

While uncertainties remain in our method, an analysis similar to that presented here could be performed for simulations with different treatments of the relevant physics of black hole accretion and feedback, star formation, or ISM processes. As the observational data improve, the comparisons presented in this paper could be used to constrain the physical prescriptions used in simulations of galaxy formation. For instance, our knowledge of possible redshift dependence in the thermal coupling η_{therm} of black hole feedback to the gas is limited. The normalization of the $M_{\text{BH}}-\sigma$ relation depends on η_{therm} for a given accretion model, and a strong increase in η_{therm} would introduce a correspondingly larger scatter in the $M_{\text{BH}}-\sigma$ relation at $z = 0$. A decrease in the thermal coupling with redshift would decrease the scatter at $z = 0$,

but in principle this effect could be counteracted if the dominant mode of black hole accretion is more efficient at higher redshifts. Better observational samples will help inform our modeling of these physics by improving constraints from the statistical moments of the $z = 0$ $M_{\text{BH}}-\sigma$ relation.

While our method for comparing evolution in the $M_{\text{BH}}-\sigma$ relation with observational constraints involves adopting a probability distribution function $P(z_f|\log M_{\text{BH}})$ relating black hole mass with a characteristic formation redshift, the general formalism does not depend on the particular choice of $P(z_f|\log M_{\text{BH}})$ or the corresponding interpretation of the quasar luminosity function. A similar analysis may be repeated for other theoretical frameworks connecting galaxy formation to SMBH growth.

The largest final black hole masses we consider are $M_{\text{BH}} \sim 3 \times 10^9 M_{\odot}$, which are produced in the mergers of the very largest galaxies in our simulations. In principle, the rarest gas-rich mergers at high redshifts could produce extraordinarily massive black holes. The upper mass limit for black holes in the simulations presented here only reflects the final potential well depth of the largest galaxies we chose to merge, as the $M_{\text{BH}}-\sigma$ relation generated by these mergers is a self-regulated process. The black holes grow in size to accommodate the growing potential foisted by star formation in the highest density regions of the galaxy during the height of the merger. As the energy input from the black hole into the surrounding gas saturates the ability of the gas contained by the potential to cool, a strong outflow is driven from the central regions, and the growth of the black hole and spheroid are truncated. There is no indication in our simulations that this process cannot continue in suitably massive gas-rich galaxy mergers to produce $\sim 10^{10} M_{\odot}$ black holes, and future work to determine the possibility of forming such black holes in galaxy mergers is planned.

However, evidence from the red sequence of the galaxy color bimodality (Strateva et al. 2001; Blanton et al. 2003; Baldry et al. 2004; Bell et al. 2004; Faber et al. 2005) suggests that the most massive galaxies are produced through the dry merging of spheroids at $z < 1$ (Bell et al. 2006; van Dokkum 2005). In this picture, $10^{10} M_{\odot}$ black holes would likely have to grow in mass, partially through binary black hole mergers. Whether black hole coalescence can occur in collisionless systems on a reasonable timescale is still an unresolved theoretical problem (e.g., Begelman et al. 1980; Milosavljevic & Merritt 2001). Cosmological simulations that include prescriptions for black hole growth may naturally account for the formation of the most massive black holes and spheroids, but even this approach will likely experience limitations due to simulated volume size, as the most massive galaxies are extremely rare. Semianalytical models that include prescriptions for black hole feedback provide another promising alternative, as such calculations can take advantage of N -body simulations such as the Millennium Run (Springel et al. 2005c) that simulate cosmological volumes with 10^{10} dark matter particles. However, the semianalytical approach may ultimately need to be calibrated against simulations such as those presented here if there is any hope of realistically capturing the complicated hydrodynamical process that generates the $M_{\text{BH}}-\sigma$ relation. The existence and possible origin of the most massive SMBHs therefore promise to be an interesting avenue of future research.

Finally, the robust nature of the $M_{\text{BH}}-\sigma$ relation produced by our simulations suggests that the merging of galaxies over cosmic time produces a relation with small intrinsic scatter, in accord with observations. The weak evolution of the calculated $M_{\text{BH}}-\sigma$ normalization implies that the small observed scatter in the $M_{\text{BH}}-\sigma$ reflects the robust physical origin of the relation (e.g.,

Haehnelt & Kauffmann 2000). While the dispersion $\Delta_{M_{\text{BH}}} = 0.25-0.3$ measured by T02 is estimated to be intrinsic to the $M_{\text{BH}}-\sigma$ relation, if the observational errors have been significantly underestimated, then our physical model may need improvement. We note that preliminary evidence of a second parameter in the $M_{\text{BH}}-\sigma$ relation (Siopis et al. 2004) may be connected to statistical variance introduced by a redshift-dependent normalization, which may take the form of a correlation with either galaxy morphology or environment. Further comparisons between the observational data and simulations could help clarify these possibilities, especially in a cosmological setting. The redshift evolution of the Faber-Jackson relation measured in the remnants may bear on observations of the fundamental plane (Dressler et al. 1987; Djorgovski & Davis 1987) and will be explored in forthcoming work.

6. SUMMARY

We calculate the $M_{\text{BH}}-\sigma$ relation produced by the merging of disk galaxies appropriate for redshifts $z = 0, 2, 3,$ and 6 using a large set of 112 hydrodynamic simulations that includes the effects of feedback from accreting SMBHs and supernovae. We develop a method for comparing the $M_{\text{BH}}-\sigma$ relation produced by simulations with existing observational constraints through the statistical moments of the measured relation, using the formalism presented by YL04, and find the simulations to be in agreement with the dispersion $\Delta_{\log M_{\text{BH}}} = 0.25-0.3$ reported by T02. The conclusions of our work are as follows.

1. The simulations suggest that the normalization of the $M_{\text{BH}}-\sigma$ relation may experience a weak evolution with redshift, while the slope is consistent with being constant near the locally observed value of $\beta \sim 4$ (Ferrarese & Merritt 2000; Gebhardt et al. 2000). As our simulations cover a wide range of virial mass, gas fraction, ISM pressurization, dark matter halo concentration, and surface mass density at each redshift, our results suggest that the physics that set the $M_{\text{BH}}-\sigma$ scaling are remarkably insensitive to the properties of progenitor galaxies in the scenario where the $M_{\text{BH}}-\sigma$ relation is created through coupled black hole and spheroid growth in galaxy mergers.

2. We demonstrate how to compare theoretical models for the $M_{\text{BH}}-\sigma$ relation that predict redshift evolution in either the slope or normalization to the observed $M_{\text{BH}}-\sigma$ relation by calculating the $z = 0$ dispersion $\Delta_{\log M_{\text{BH}}}$ of the relation, given a functional form for the evolution and a probability distribution function $P(z_f|\log M_{\text{BH}})$ that relates black hole mass to a characteristic formation redshift. Adopting a model for $P(z_f|\log M_{\text{BH}})$ from H06a, we calculate the allowed strength of redshift evolution given power-law, redshift evolution in either normalization or slope, consistent with the observed scatter at $z = 0$. The modest normalization evolution calculated by our simulations produces a scatter similar to that observed. We demonstrate how redshift evolution in the $M_{\text{BH}}-\sigma$ relation introduces mass-dependent dispersion and skewness about the average relation, and show how these statistical moments can be used to differentiate theoretical models for the $M_{\text{BH}}-\sigma$ relation that predict distinct redshift evolutions.

3. We relate our simulations to observations of the $M_{\text{BH}}-\sigma$ relation in AGNs at redshifts $z > 0$ and, given the observational and theoretical uncertainties, find the properties of our inactive remnants to be more consistent with the redshift-independent $M_{\text{BH}}-\sigma$ relation measured by Shields et al. (2003) than the claims of Treu et al. (2004) and Walter et al. (2004) that SMBHs may form earlier than galactic spheroids. We show that if the offset $\delta \log \sigma = -0.16$ in the $M_{\text{BH}}-\sigma$ relation measured by Treu et al.

(2004) for AGNs at $z = 0.37$ is attributed to a power-law evolution in the normalization of the velocity dispersion as $\sigma(z) \propto \sigma(z=0)(1+z)^\xi$, the resultant scatter expected in the $z = 0$ $M_{\text{BH}}-\sigma$ relation would be much larger than is observed. Additional comparisons between the active phase of our merger simulations and the observations of active galaxies are planned in future work.

4. Our simulations provide additional motivation for future observations of high-redshift normal galaxies using the next generation of large telescopes for the purpose of constraining the evolution of the cosmic black hole population with time. The planned 20–30 m class telescopes with infrared spectrographs should be able to measure central stellar velocity dispersions in galaxies to $z \sim 3$. Our simulations can be used to connect those measurements to estimates for the SMBH mass function and the distribution of black hole formation redshifts $P(z_f | \log M_{\text{BH}})$. A complete census of the cosmic black hole population will require measurements of the spheroidal population at high redshifts and will serve as important input into structure formation theories that account for the effects of black hole feedback on normal galaxies.

With a method for constraining theories of the $M_{\text{BH}}-\sigma$ relation with the statistical moments of the local $M_{\text{BH}}-\sigma$ relation based on their predictions for redshift evolution in the relation, future opportunities for direct comparisons between observations and theoretical models should be plentiful. As the statistics of the observational results improve, the theoretical models will be able to adjust their physical prescriptions to better accommodate empirical constraints. Research into the $M_{\text{BH}}-\sigma$ relation should then continue to prove an important area of interest for future efforts to construct a more complete theory of galaxy formation.

We acknowledge the helpful comments of the referee, Doug Richstone, that helped improve the presentation and clarity of our results. This work was supported in part by NSF grants ACI 96-19019, AST 00-71019, AST 02-06299, and AST 03-07690, and NASA ATP grants NAG5-12140, NAG5-13292, and NAG5-13381. The simulations were performed at the Center for Parallel Astrophysical Computing at the Harvard-Smithsonian Center for Astrophysics.

REFERENCES

- Adams, F. C., Graff, D. S., Mbonye, M., & Richstone, D. O. 2003, *ApJ*, 591, 125
- Adams, F. C., Graff, D. S., & Richstone, D. O. 2001, *ApJ*, 551, L31
- Andersen, T. E., et al. 2004, *Proc. SPIE*, 5489, 407
- Archibald, E. N., Dunlop, J. S., Jimenez, R., Friaça, A. C. S., McLure, R. J., & Hughes, D. H. 2002, *MNRAS*, 336, 353
- Baes, M., Buyle, P., Hau, G. K. T., & Dejonghe, H. 2003, *MNRAS*, 341, L44
- Balberg, S., & Shapiro, S. L. 2002, *Phys. Rev. Lett.*, 88, 101301
- Baldry, I. K., Glazebrook, K., Brinkmann, J., Ivezić, Z., Lupton, R. H., Nichol, R. C., & Szalay, A. S. 2004, *ApJ*, 600, 681
- Begelman, M. C., Blandford, R. D., & Rees, M. J. 1980, *Nature*, 287, 307
- Bell, E., et al. 2004, *ApJ*, 608, 752
- . 2006, *ApJ*, 640, 241
- Bernardi, M., et al. 2003, *AJ*, 125, 1866
- Blanton, M., et al. 2003, *ApJ*, 594, 186
- Bondi, H. 1952, *MNRAS*, 112, 195
- Bondi, H., & Hoyle, F. 1944, *MNRAS*, 104, 273
- Boyle, B. J., Shanks, T., Croom, S. M., Smith, R. J., Miller, L., Loaring, N., & Heymans, C. 2000, *MNRAS*, 317, 1014
- Bromley, J. M., Somerville, R. S., & Fabian, A. C. 2004, *MNRAS*, 350, 456
- Bullock, J. S., Kolatt, T. S., Sigad, Y., Somerville, R. S., Kravtsov, A. V., Klypin, A. A., Primack, J. R., & Dekel, A. 2001, *MNRAS*, 321, 559
- Burkert, A., & Silk, J. 2001, *ApJ*, 554, L151
- Ciotti, L., & van Albada, T. S. 2001, *ApJ*, 552, L13
- Cowie, L. L., Barger, A. J., Bautz, M. W., Brandt, W. N., & Garmire, G. P. 2003, *ApJ*, 584, L57
- Cox, T. J., Di Matteo, T., Hernquist, L., Hopkins, P. F., Robertson, B., & Springel, S. 2006, *ApJ*, submitted (astro-ph/0504156)
- Dierickx, P., et al. 2004, *Proc. SPIE*, 5489, 391
- Di Matteo, T., Croft, R. A. C., Springel, V., & Hernquist, L. 2003, *ApJ*, 593, 56
- . 2004, *ApJ*, 610, 80
- Di Matteo, T., Springel, V., & Hernquist, L. 2005, *Nature*, 433, 604
- Djorgovski, S., & Davis, M. 1987, *ApJ*, 313, 59
- Dressler, A., Lynden-Bell, D., Burstein, D., Davies, R. L., Faber, S. M., Terlevich, R., & Wegner, G. 1987, *ApJ*, 313, 42
- Eckart, A., & Genzel, R. 1997, *MNRAS*, 284, 576
- Faber, S. M., & Jackson, R. E. 1976, *ApJ*, 204, 668
- Faber, S. M., et al. 1997, *AJ*, 114, 1771
- . 2005, *ApJ*, submitted (astro-ph/0506044)
- Fabian, A. C. 1999, *MNRAS*, 308, L39
- Ferrarese, L. 2002, *ApJ*, 578, 90
- Ferrarese, L., & Merritt, D. 2000, *ApJ*, 539, L9
- Gebhardt, K., et al. 2000, *ApJ*, 539, L13
- . 2003, *ApJ*, 597, 239
- Ghez, A. M., Klein, B. L., Morris, M., & Becklin, E. E. 1998, *ApJ*, 509, 678
- Gingold, R. A., & Monaghan, J. J. 1977, *MNRAS*, 181, 375
- Granato, G. L., Silva, L., Monaco, P., Pazuozzo, P., Salucci, P., De Zotti, G., & Danese, L. 2001, *MNRAS*, 324, 757
- Haehnelt, M. G., & Kauffmann, G. 2000, *MNRAS*, 318, L35
- Haiman, Z., & Loeb, A. 1998, *ApJ*, 503, 505
- Hernquist, L. 1990, *ApJ*, 356, 359
- Ho, L. C., Sarzi, M., Rix, H., Shields, J. C., Rudnick, G., Filippenko, A. V., & Barth, A. J. 2002, *PASP*, 114, 137
- Hopkins, P. F., Hernquist, L., Cox, T. J., Di Matteo, T., Martini, P., Robertson, B., & Springel, S. 2005a, *ApJ*, 630, 705
- . 2005b, *ApJ*, 630, 716
- . 2005c, *ApJ*, 632, 81
- Hopkins, P. F., Hernquist, L., Cox, T. J., Di Matteo, T., Robertson, B., & Springel, S. 2006a, *ApJS*, 163, 1 (H06a)
- . 2006b, *ApJ*, 639, 700
- Hopkins, P. F., Hernquist, L., Cox, T. J., Robertson, B., & Springel, S. 2006c, *ApJS*, 163, 50
- Hopkins, P. F., Hernquist, L., Martini, P., Cox, T. J., Robertson, B., Di Matteo, T., & Springel, S. 2005d, *ApJ*, 625, L71
- Hoyle, F., & Lyttleton, R. A. 1939, *Proc. Cambridge Philos. Soc.*, 35, 405
- Iye, M., et al. 2004, *Proc. SPIE*, 5489, 417
- Johns, M., Angel, J. R. P., Sheckman, S., Bernstein, R., Fabricant, D. G., McCarthy, P., & Phillips, M. 2004, *Proc. SPIE*, 5489, 441
- Kauffmann, G., & Haehnelt, M. 2000, *MNRAS*, 311, 576
- Kazantzidis, S., et al. 2005, *ApJ*, 623, L67
- King, A. 2003, *ApJ*, 596, L27
- Kormendy, J., & Richstone, D. 1995, *ARA&A*, 33, 581
- Lidz, A., Hopkins, P. F., Cox, T. J., Hernquist, L., & Robertson, B. 2006, *ApJ*, 641, 41
- Lucy, L. B. 1977, *AJ*, 82, 1013
- MacMillan, J. D., & Henriksen, R. N. 2002, *ApJ*, 569, 83
- Magorrian, J., et al. 1998, *AJ*, 115, 2285
- Marconi, A., & Hunt, L. K. 2003, *ApJ*, 589, L21
- McKee, C. F., & Ostriker, J. P. 1977, *ApJ*, 218, 148
- Menci, N., Cavaliere, A., Fontana, A., Giallongo, E., Poli, F., & Vittorini, V. 2003, *ApJ*, 587, L63
- Menou, K., Haiman, Z., & Narayanan, V. K. 2001, *ApJ*, 558, 535
- Milosavljevic, M., & Merritt, D. 2001, *ApJ*, 563, 34
- Miralda-Escudé, J., & Kollmeier, J. A. 2005, *ApJ*, 619, 30
- Miyoshi, M., Moran, J., Herrnstein, J., Greenhill, L., Nakai, N., Diamond, P., & Inoue, M. 1995, *Nature*, 373, 127
- Mo, H. J., Mao, S., & White, S. D. M. 1998, *MNRAS*, 295, 319
- Monaco, P., Salucci, P., & Danese, L. 2000, *MNRAS*, 311, 279
- Murray, N., Quataert, E., & Thompson, T. A. 2005, *ApJ*, 618, 569
- Navarro, J. F., Frenk, C. S., & White, S. D. M. 1997, *ApJ*, 490, 493
- Nelson, C. H. 2000a, *ApJ*, 544, L91
- Nelson, C. H., & Whittle, M. 1996, *ApJ*, 465, 96
- Nelson, J. E. 2000b, *Proc. SPIE*, 4004, 282
- Nipoti, C., Londrillo, P., & Ciotti, L. 2003, *MNRAS*, 342, 501
- Richstone, D., et al. 1998, *Nature*, 395, A14
- Robertson, B., Hernquist, L., Bullock, J. S., Cox, T. J., Di Matteo, T., Springel, V., & Yoshida, N. 2006, *ApJ*, submitted (astro-ph/0503369)
- Robertson, B., Yoshida, N., Springel, V., & Hernquist, L. 2004, *ApJ*, 606, 32

- Rusin, D., Keeton, C. R., & Winn, J. N. 2005, *ApJ*, 627, L93
- Sanders, D. B., & Mirabel, I. F. 1996, *ARA&A*, 34, 749
- Sanders, D. B., Soifer, B. T., Elias, J. H., Madore, B. F., Matthews, K., Neugebauer, G., & Scoville, N. Z. 1988, *ApJ*, 325, 74
- Sazonov, S. Y., Ostriker, J. P., Ciotti, L., & Sunyaev, R. A. 2005, *MNRAS*, 358, 168
- Schmidt, M., Schneider, D. P., & Gunn, J. E. 1995, *AJ*, 110, 68
- Shields, G. A., Gebhardt, K., Salviander, S., Wills, B. J., Xie, B., Brotherton, M. S., Yuan, J., & Dietrich, M. 2003, *ApJ*, 583, 124
- Siegel, M. H., Majewski, S. R., Reid, I. N., & Thompson, I. B. 2002, *ApJ*, 578, 151
- Silk, J., & Rees, M. J. 1998, *A&A*, 331, L1
- Siopis, C., et al. 2004, *AAS Mtg. Abstr.*, 205
- Smail, I., Ivison, R. J., & Blain, A. W. 1997, *ApJ*, 490, L5
- Springel, V. 2006, *MNRAS*, in press
- Springel, V., Di Matteo, T., & Hernquist, L. 2005a, *ApJ*, 620, L79
- . 2005b, *MNRAS*, 361, 776
- Springel, V., & Hernquist, L. 2002, *MNRAS*, 333, 649
- . 2003, *MNRAS*, 339, 289
- Springel, V., Yoshida, N., & White, S. D. M. 2001, *NewA*, 6, 79
- Springel, V., et al. 2005c, *Nature*, 435, 629
- Steffen, A. T., Barger, A. J., Cowie, L. L., Mushotzky, R. F., & Yang, Y. 2003, *ApJ*, 596, L23
- Strateva, I., et al. 2001, *AJ*, 122, 1861
- Su, D., Wang, Y., & Cui, X. 2004, *Proc. SPIE*, 5489, 429
- Toomre, A. 1964, *ApJ*, 139, 1217
- . 1977, in *Evolution of Galaxies and Stellar Populations*, ed. B. M. Tinsley & R. B. Larson (New Haven: Yale Univ. Obs.), 401
- Tremaine, S., et al. 2002, *ApJ*, 574, 740 (T02)
- Treu, T., Malkan, M. A., & Blandford, R. D. 2004, *ApJ*, 615, L97
- Treu, T., Stiavelli, M., Møller, P., Casertano, S., & Bertin, G. 2001, *MNRAS*, 326, 221
- van Dokkum, P. G. 2005, *AJ*, 130, 2647
- van Dokkum, P. G., & Stanford, S. A. 2003, *ApJ*, 585, 78
- Vestergaard, M. 2004, *ApJ*, 601, 676
- Vitvitska, M., Klypin, A. A., Kravtsov, A. V., Wechsler, R. H., Primack, J. R., & Bullock, J. S. 2002, *ApJ*, 581, 799
- Volonteri, M., Haardt, F., & Madau, P. 2003, *ApJ*, 582, 559
- Walter, F., Carilli, C., Bertoldi, F., Menten, K., Cox, P., Lo, K. Y., Fan, X., & Strauss, M. A. 2004, *ApJ*, 615, L17
- Wandel, A. 2002, *ApJ*, 565, 762
- Wandel, A., Peterson, B. M., & Malkan, M. A. 1999, *ApJ*, 526, 579
- Wyithe, J. S. B. 2006, *MNRAS*, 365, 1082
- Wyithe, J. S. B., & Loeb, A. 2003, *ApJ*, 595, 614
- Yu, Q., & Lu, Y. 2004, *ApJ*, 610, 93 (YL04)
- Yu, Q., & Tremaine, S. 2002, *MNRAS*, 335, 965